HHS Public Access

Author manuscript

DNA Repair (Amst). Author manuscript; available in PMC 2020 September 01.

Published in final edited form as:

DNA Repair (Amst). 2019 September ; 81: 102650. doi:10.1016/j.dnarep.2019.102650.

Quantitating repair protein accumulation at DNA lesions: Past, Present, and Future

Jyothi Mahadevan[1,†], **Samuel Bowerman**[1,2,†], **Karolin Luger**[1,2,*]

[1]Department of Biochemistry, University of Colorado Boulder, Boulder, CO 80309, USA

[2]Howard Hughes Medical Institute, University of Colorado Boulder, Boulder, CO 80309, USA

Abstract

All organisms must protect their genome from constantly occurring DNA damage. To this end, cells have evolved complex pathways for repairing sites of DNA lesions, and multiple *in vitro* and *in vivo* techniques have been developed to study these processes. In this review, we discuss the commonly used laser microirradiation method for monitoring the accumulation of repair proteins at DNA damage sites in cells, and we outline several strategies for deriving kinetic models from such experimental data. We discuss an example of how *in vitro* measurements and *in vivo* microirradation experiments complement each other to provide insight into the mechanism of PARP1 recruitment to DNA lesions. We also discuss a strategy to combine data obtained for the recruitment of many different proteins in a move toward fully quantitating the spatiotemporal relationships between various damage responses, and we outline potential venues for future development in the field.

Keywords

Laser microirradiation; kinetic modelling; accumulation; recruitment to DNA damage sites; DNA repair protein; PARP1; Q-FADD

1. Introduction

Throughout the lifetime of an organism, its genetic material is constantly assaulted by many endogenous and exogenous DNA-damaging agents. Damage to DNA can result in simple base substitutions or more complex changes such as formation of single or double strand DNA breaks (SSBs or DSBs). SSBs commonly arise due to the spontaneous oxidative action of endogenously-formed free radicals, ultimately resulting in a break in one of the two strands of the DNA double helix [1,2]. Such DNA lesions can cause obstruction of the transcription and/or replication machineries. Indeed, if SSBs are missed by the surveillance

*To whom correspondence should be addressed. Tel: +1 303-735-6689; karolin.luger@.colorado.edu.
†Authors contributed equally to this work

Conflict of interest statement: None declared

machinery and remain unrepaired in cycling cells, DNA replication forks can collapse in S-phase cells, resulting in the conversion of SSBs to DSBs. Another direct cause of DSBs is exposure to ionizing radiation. When cells fail to repair DSBs, untoward consequences such as genomic instability and cell death will occur. All living organisms have evolved highly coordinated mechanisms for repairing damaged DNA, thereby safeguarding genome integrity [3–6]. These processes are the subject of intense study.

Early in the process of SSB repair (SSBR), poly (ADP-ribose) polymerase 1 (PARP1) rapidly accumulates at sites of DNA damage. PARP1 is a molecular sensor of various forms of damaged DNA and is enzymatically activated upon binding to damage sites. This results in the rapid synthesis of negatively charged poly-ADP ribose (PAR) chains onto itself and other target proteins [7, 8]. These PAR chains, consisting of up to several hundred ADP-ribose molecules in a branched conformation, recruit other repair proteins such as X-ray repair cross-complementing protein 1 (XRCC1), ligase 3, polynucleotide kinase 3'-phosphate (PNKP), aprataxin, and DNA polymerase β to mediate SSBR [9–11]. DSB repair (DSBR) occurs via one of two main pathways: homologous recombination (HR), or classical non-homologous end joining (c-NHEJ). DSBR usually activates a process known as 'end resection', wherein the DNA ends undergo nucleolytic cleavage from the 5' to 3' end to form a long ssDNA segment on the 3' strand. Repair of DSBs by HR is favored when DNA end resection occurs since the long 3' ssDNA can invade the homologous DNA strand. This process occurs predominantly in the late S and G2 phases of the cell cycle, when a sister chromatid becomes available [12]. HR is initiated by recruitment of meiotic recombination 11 (MRE11) and ataxia telangiectasia mutated (ATM) to DSBs. The recombinase RAD51 is responsible for strand invasion, ultimately leading to the completion of the repair process by RAD52, RAD54 and Polδ [13]. Alternatively, in the absence of a homologous sequence or end resection, the c-NHEJ pathway is favored. In this process, the DNA ends are directly ligated, which requires factors such as Ku70/80, DNA-PKcs and DNA ligase IV [14–16]. The absence of Ku70/80 is compensated by PARP1 recruitment to locations of DSBs [17]. *In vitro* and *in vivo* studies conducted over the past fifty years have revealed that most of the above listed repair proteins often participate in multiple DNA repair pathways; however, the exact mechanisms of how the requisite cohort of proteins assemble to perform their activities to effectively repair diverse DNA lesions is yet to be fully determined.

A number of *in vitro* and *in vivo* strategies are currently utilized to dissect DNA damage repair, and a complete understanding of these mechanisms requires the use of multiple experimental approaches. *In vitro* approaches include, but are not limited to, the use of fluorescence polarization, Fluorescence Resonance Energy Transfer (FRET), and stopped-flow anisotropy assays to study the mechanisms governing association (and dissociation) of repair factors with model DNA fragments, plasmids, or nucleosomes [18, 19]. These experiments provide detailed insights into the molecular behavior of individual or small subsets of proteins that participate in DNA repair. Several *in vivo* methods such as PCR-based assays, the 'comet assay', and TUNEL assays can quantitate the degree of cellular DNA damage [20]. Fluorescence techniques, e.g. Fluorescence Recovery After Photobleaching (FRAP), Fluorescence Loss In Photobleaching (FLIP), Fluorescence Correlation Spectroscopy (FCS), and laser microirradiation, can be used to monitor repair protein kinetics in a nuclear context and can be interpreted in conjunction with the

aforementioned *in vitro* measurements. In FRAP and FLIP, a small region within the cell is rapidly photobleached by a short pulse of high intensity radiation, and the recovery of fluorescently-tagged protein to the region (FRAP) or depletion of fluorescence outside the region (FLIP) is examined by time-lapse microscopy. On the other hand, FCS measures the change in fluorescence intensity as the protein of interest traverses a femtoliter volume within the cell [21–30]. While FRAP, FLIP, and FCS are typically designed to quantitate protein movement independent of DNA damage, laser microirradiation specifically focuses on the process of repair protein accumulation at DNA lesions [31–34].

Recent massive efforts have been placed on using laser microirradiation to understand the spatiotemporal details of repair protein accumulation at sites of DNA damage [35, 36]. In this approach, damage foci are induced by short wavelength (355 nm – 400 nm) light, and the accumulation of repair proteins to the irradiated site is detected either by immunofluorescence or by live-cell tracking of the fluorescently-tagged protein(s) of interest. Cells can be pre-sensitized by the addition of halogenated nucleotide analogs, such as bromodeoxyuridine (BrdU), or DNA-intercalating Hoechst dyes, which enables the use of 405 nm laser lines typically available on standard laser scanning confocal microscopes. Laser microirradiation is a powerful method for monitoring the kinetics of recruitment and the sequence of assembly of repair protein complexes on damaged DNA [16, 35–37]. However, a major limitation for this approach to reach its full potential has been the lack of reliable methods to derive meaningful quantitative information from imaging data. In this review, we highlight the widespread use of laser microirradiation over the last four decades, and we describe various methods currently in use for analyzing the accumulation of DNA repair proteins. In addition, we suggest approaches by which quantitation could be improved.

2. A Brief History of laser-induced DNA Damage Studies

One of the earliest reports for the use of intense light to induce DNA damage *in vivo* dates back to 1969 (Fig. 1). Here, an argon ion laser was used to induce lesions on pre-determined sites on chromosomes of salamander lung cells stained with acridine orange, and it was found that cells could survive localized doses of microirradiation and continue to divide [38]. In 1978, another group used a mercury arc lamp to generate 313 nm ultraviolet (UV) rays to introduce DSBs in bromouracil-substituted cellular DNA in *E. coli* cells. Sensitivity of *E. coli* cells to photolysis increased linearly with the number of bromouracil molecules incorporated into the DNA [39]. In a modification of this method reported two years later, Hoechst 33258 stain was used to enhance the photolytic effect of BrdU treatment in human fibroblasts irradiated with 365 nm light. This wavelength of UV-light presented an advantage over the earlier approach that used 313 nm light since many aromatic ring-containing carcinogens form DNA adducts that strongly absorb 313 nm light [40]. In 1993, Limoli and Ward quantitated the formation of DSBs in cellular DNA subjected to photolysis using a combination of BrdU, Hoechst 33258, and near-visible UV light using the alkaline filter elution method [41]. In the following years, multiple groups continued to make improvements to this approach. These efforts enabled the visualization of γ-H2AX foci generated in human cells by indirect immunofluorescence by Rogakou et al. Here, the irradiating laser was guided along a pre-drawn path using an analog joystick [42]. To

understand the significance of γ-H2AX in the DNA damage signaling process, Celeste et al. introduced DSBs in Hoechst-stained mouse embryonic fibroblasts (MEFs) using a laser-dissecting microscope (337 nm). This study suggested that H2AX phosphorylation was not required for formation of damage foci but was necessary for the concentration of repair factors like NBS1, 53BP1, and BRCA1 at DNA lesions. These efforts together established γ-H2AX as a DSB marker in the DNA repair field [43].

In following years, the use of a laser scanning microscope to generate a precise path of DNA damage followed by real time live-cell imaging became a widely used approach in the field of DNA repair. Concomitantly, the biological functions of many repair proteins including NBS1, XRCC1, PARP1, and PARP2 were uncovered, resulting in a clearer understanding of the DNA repair signaling process [31,44, 45]. Since then, longer wavelengths of light (365-405 nm) have been utilized for introducing DSBs in mammalian cells stained with Hoechst dyes to compare the functions of repair proteins that participate in different repair mechanisms [31, 46, 47]. Some groups also began using laser microirradiation without prior chemical pre-sensitization in an attempt to investigate particular kinds of DNA lesions [48, 49]. In fact, DNA sensitization is not required when high-energy multiphoton near-infrared (NIR) lasers are used to inflict DNA damage; however, such high energies may ultimately cause premature cell death [48–51]. It is important to note that the type of DNA lesions induced and the way these lesions are processed could vary with the choice of the chemical sensitizer, the wavelength of light, and the duration of the pulse. These variations result in formation of a poorly understood mixture of DNA damage types such as pyrimidine dimers, inappropriate base modifications and inter-strand crosslinks [48, 52]. This heterogeneity has deterred researchers from comparing their findings to those of other groups, thereby limiting the ability to comprehend the interplay between different repair pathways.

Laser microirradiation has also been used as a tool to investigate remodeling of chromatin structure that accompanies the DNA repair process [53, 54]. The dynamic alteration of chromatin architecture that occurs as a consequence of disruption of DNA double-helical structure has been visualized using a photoactivatable version of GFP-tagged histone H2B (PAGFP-H2B) [55]. The 364 nm laser line was used to simultaneously induce DSBs and photoconvert the PAGFP to the active form. This study concluded that local chromatin undergoes rapid ATP-dependent decondensation immediately after the DNA damaging event [55], and another group independently established that this process was mediated by PARP1-dependent PARylation [56].

The last five years have witnessed an insurgence of information regarding the recruitment of several DNA damage response (DDR) proteins to laser-induced damage sites. In 2015, Izhar et al. performed a focused screen for proteins that arrived at DNA lesions post UV laser microirradiation [37]. Their work revealed that multiple families of transcription factors localized at damage sites in a DNA binding domain-dependent and/or a PARP-dependent manner [37]. In another study, Kochan et al. revisited numerous DSBR-related reports and performed a systematic analysis of laser-microirradiation data generated for 79 repair proteins to obtain insight into the spatiotemporal details of DSBR [36]. More recently, in 2018, Aleksandrov et al. carried out the mammoth task of measuring and mathematically modeling the recruitment kinetics of 70 proteins at laser-induced damage sites both in the

presence and absence of a PARP inhibitor in living HeLa Kyoto cell lines [35]. This work provided information on the timing and sequence of arrival and removal of repair proteins at complex DNA lesions under similar experimental conditions [35]. Since then, many more research groups have relied on the powerful approach of laser microirradiation to probe the kinetics of recruitment of several repair proteins and their mutant counterparts [18, 33, 57–60].

3. Methods for quantitative analysis of laser microirradiation data

Laser microirradiation experiments are most frequently described by a fluorescence intensity time series for the region of interest after the damage event (Fig. 2). Such graphs depict the accumulation (and subsequent dissipation) of fluorescently labeled repair proteins at laser-induced damage sites. In practice, intensity values are generated from raw images using proprietary (Nikon Elements, ZEN) or publicly available (ImageJ) [61] imaging software packages, and each point within the timeseries is generally normalized to pre-irradiation values and corrected for background fluorescence. Furthermore, the fluorescence loss that occurs over the course of the experiment (photobleaching) can also be accounted for. A common practice in the field is to average data from 10-20 independently damaged nuclei and report a mean value with error for each time point within the curve [31,62, 63].

Currently, one of the most widely used methods for quantitating accumulation timescales for various DNA repair proteins is to report the time required for half of the maximum accumulation to occur ($t_{1/2}$). This is the quickest form of analysis currently in use, and it is a reliable method for comparing the accumulation of multiple repair proteins within a single nucleus. However, when accumulation kinetics are being compared between distinct nuclei, it is important to note that $t_{1/2}$ is strongly influenced by the shape and size of the nucleus under examination [64] . Therefore, averaging multiple timeseries as part of a single kinetics population is not necessarily correct, as populations with diverse features (such as bimodality) cannot be solely assessed from a single mean and standard deviation [64–66]. Moreover, while $t_{1/2}$ can be used to swiftly assess the speed of protein accumulation, it provides little information on the underlying physics of the protein transport process (simple, facilitated or anomalous diffusion).

An additional layer of quantitation can be obtained from accumulation data by fitting it to an exponential model [$I(t) = A(1-e^{-kt})$], where the accumulation rate constants (k) can be derived directly from the equation of best fit. Many proteins can be described by a first-order exponential fit [36, 67], but some proteins may require additional exponential terms [35, 68]. In these cases, the first-order term may describe a phase of rapid accumulation, whereas a second-order exponential would describe accumulation at longer timescales. Another method based in exponential fitting is the “Consecutive Chain Reactions” (CRC) model employed by Aleksandrov et al. to rationalize both protein accumulation and removal as a series of consecutive reactions, each with its own characteristic rate [35]. These approaches provide quantitative information about the underlying kinetic rates of accumulation, allowing for potential comparisons between the activation of different repair proteins. If these experiments are performed under similar conditions, one can actually determine the sequence of arrival to damage sites for a collection of proteins [35]. Nonetheless,

exponential fitting still suffers from similar restrictions as does $t_{1/2}$ evaluation, since these models are both affected by nuclear size and shape [64]. As a result, it is difficult to deduce a direct and meaningful physical interpretation of the diffusion process involved, especially when multiple nuclei are averaged to provide a single intensity timeseries [64]. Furthermore, it is important to exercise caution and avoid the spurious use of multiple exponentials for fitting accumulation curves, as the inclusion of unwarranted extra parameters to the model could lead to arbitrarily strong fits to the experimental data and lead to a potential misinterpretation of the underlying biological processes [69].

Recent efforts in our own lab have focused on developing a quantitative method to explain repair protein accumulation at DNA lesions that recognizes the role of nuclear shape and size. Quantitation of Fluorescence Accumulation after DNA Damage (Q-FADD) assumes that repair proteins move within the nucleus by simple free diffusion [64], as previous studies have shown that many proteins may navigate to sites of DNA damage through a free diffusion process [70–73]. Q-FADD utilizes a Monte Carlo simulation to describe molecular motion within a two-dimensional, nucleus-shaped grid to track protein accumulation within the defined region-of-interest (ROI), i. e. the DNA damage site. Originally, Q-FADD was developed to explain the diffusive behaviors of PARP1, PARP2, and Histone Parylation Factor 1 (HPF1), a new player in the DNA repair field [64, 74, 75]. Notably, the effective diffusion coefficient (D_{eff}) derived from Q-FADD can be directly compared to D_{eff} from other methods, such as FRAP and FCS [76]. While Q-FADD is able to provide D_{eff} values in agreement with these other methods, levels of information such as dwell times and binding kinetics are integrated into a mobility fraction parameter, and derivation of these underlying properties requires orthogonal information from separate techniques.

We have employed Q-FADD to elucidate the dynamic mechanism of PARP1 recruitment *in vivo* [18]. Indeed, PARP1 is among the fastest proteins recruited to sites of DNA damage [35], but the means by which PARP1 so rapidly seeks out sections of DSBs was largely unknown. *In vitro* kinetics work showed that purified PARP1 rapidly binds to DNA ends and that the release of bound DNA requires formation of a ternary complex with a second piece of DNA [18]. These data suggested that PARP1 navigates DNA through an intersegment transfer scheme, similar to how a child navigates playground monkey bars by a hand-over-hand exchange. Mutation studies identified the WGR domain of PARP1 as responsible for this action, as W589A mutation or WGR domain deletion prevented ternary complex formation. Similarly, Q-FADD analysis showed that W589A mutation significantly decreased the observed D_{eff} value describing PARP1 accumulation (3.7 ± 0.6 $\mu m^2/s$ vs 2.1 ± 0.2 $\mu m^2/s$, $p = 0.0094$), providing *in vivo* evidence for the “monkey-bar” mechanism of PARP1 mobility and confirming the important role of the WGR domain for biological efficacy (Fig. 3). As the mechanism was proposed by *in vitro* observations and confirmed through *in vivo* microirradiation quantitation, this study provides a classic example for the enhanced level of biological insight that can be gained from the combined use of quantitative *in vivo* and *in vitro* techniques.

Until now, we have focused on the importance of quantitating microirradiation data for individual proteins. However, comparative analysis of multiple repair proteins also benefits from more quantitative approaches. For example, the recent study by Aleksandrov et al. used

a divisive clustering algorithm (DIANA) to group a wide range of proteins in different arrival and removal clusters according to their measured $t_{1/2}$ values [35]. From their results, they were able to show that when proteins are clustered according to their accumulation timescales, members of the same response pathway can be found within the same arrival cluster. By comparing to a library of known protein-protein interactions, they were also able to identify proteins that regulate DNA damage repair between pathways and timescales. Upon addition of PARP inhibitors, it was observed that proteins from PARP-independent pathways experienced changes in both their accumulation and depletion rates. Thus, inhibiting one repair pathway can cause the cell to alter priority in favor of another. Moreover, these results suggest that complex crosstalk may exist between various repair responses. As such, Aleksandrov et al. have demonstrated the importance of using several levels of quantitation to promote better understanding of the cellular response to DNA damage.

4. Perspective/Future Directions

Here, we have revisited the 50-year history of the laser microirradiation field, and we have highlighted several techniques that are currently used for quantitating microirradiation observations. Recent advancements in fluorescent labeling [77, 78]. as well as superior imaging systems and user-friendly computational tools have resulted in the ability to derive deeper biophysical knowledge from laser microirradiation experiments. Since robust modeling of irradiation data can provide insight into protein transport mechanisms, distribution of mobile and immobile protein populations, as well as (dis)association constants, continued emphasis should be placed on using these enhanced resources to develop even more robust quantitative modeling approaches, similar to current developments in methods such as FRAP and FCS [72, 79–81].

While the quantitation methods discussed in this review provide a range of insights to biological processes, differences in results obtained from various experimental approaches are still difficult to interpret [24] . First, the presence of the fluorescence tag may affect diffusion kinetics in a protein-specific manner [82]. Additionally, proteins could have smaller D_{eff} values or accumulation rate constants because they bind to other proteins or immobile chromatin structures, whereas proteins with a larger accumulation rate or D_{eff} value may encounter fewer binding and unbinding events. In this way, quantitative models should still be interpreted with caution and supplemented with other measurements, although future developments in modeling techniques could potentially be extended to include prediction of protein residence times on chromatin and thereby recover this information.

Improvements to quantitative *in vivo* modeling should also not stop at the per-protein or single timeseries level. While the previously discussed study by Aleksandrov et al. was conducted on $t_{1/2}$ values [35], it is important to note that methods such as DIANA clustering are not restricted to $t_{1/2}$ measures alone. This type of analysis can be used to compare accumulation rates from exponential fits, as well as D_{eff} values from Q-FADD analyses. Moreover, there are a variety of clustering algorithms one might employ. The DIANA method is a divisive form of hierarchical clustering, where clusters are formed by iteratively

separating proteins from a master family, but one could also cluster proteins in an agglomerative manner, where proteins are iteratively merged from individuals in to clusters instead of divided from a larger pool [83]. Beyond hierarchical schemes, centroid-based measures like the k-means method [84] or density-based methods such as DBSCAN [85] provide alternative approaches to characterizing pathways of DNA damage response from microirradiation data. In this way, through rigorous quantitation at multiple levels, the cellular response to DNA damage events can ultimately be fully understood.

Acknowledgement

We thank Johannes Rudolph for critical reading of the manuscript. JM and KL are supported by National Institutes of Health – National Cancer Institute (R01 CA218255) and the University of Colorado Cancer Center (Pilot Funding Grant ST63501792). Members of the Luger Lab are also supported by the Howard Hughes Medical Institute.

ABBREVIATIONS

SSBs	Single strand breaks
SSBR	Single strand break repair
DSBs	Double strand breaks
DSBR	Double strand break repair
PARP1/2	Poly ADP-ribose polymerase 1/2
PAR	Poly ADP-ribose
XRCC1	X-ray repair cross-complementing protein 1
PNKP	polynucleotide kinase 3’-phosphate
HR	homologous recombination
c-NHEJ	classical non-homologous end joining
ssDNA	single stranded DNA
DNA-PKcs	DNA-dependent protein kinase, catalytic subunit
FRET	Fluorescence Resonance Energy Transfer
MRE11	meiotic recombination 11
ATM	ataxia telangiectasia mutated
TUNEL	terminal deoxynucleotidyl transferase dUTP nick-end labeling
FRAP	Fluorescence Recovery After Photobleaching
FLIP	Fluorescence Loss In Photobleaching
FCS	Fluorescence Correlation Spectroscopy

BrdU	bromodeoxyuridine
UV	ultraviolet
NBS1	Nibrin
NIR	near-infrared
PAGFP-H2B	photoactivatable GFP-tagged histone H2B
DDR	DNA damage response
CRC	Consecutive Chain Reactions
Q-FADD	Quantitation of Fluorescence Accumulation after DNA Damage
ROI	region-of-interest
HPF1	Histone Parylation Factor 1
$\mathbf{D_{eff}}$	effective diffusion coefficient
DIANA	Divisive Analysis
DBSCAN	density-based scan

References

1. Caldecott KW, Mammalian DNA single-strand break repair: an X-ra(y)ted affair. Bioessays, 2001 23(5): p. 447–55. [PubMed: 11340626]
2. Abbotts R and Wilson DM 3rd, Coordination of DNA single strand break repair. Free Radic Biol Med, 2017 107: p. 228–244. [PubMed: 27890643]
3. Zhou BB and Elledge SJ, The DNA damage response: putting checkpoints in perspective. Nature, 2000 408(6811): p. 433–9. [PubMed: 11100718]
4. Sancar A, et al., Molecular mechanisms of mammalian DNA repair and the DNA damage checkpoints. Annu Rev Biochem, 2004 73: p. 39–85. [PubMed: 15189136]
5. Sirbu BM and Cortez D, DNA damage response: three levels of DNA repair regulation. Cold Spring Harb Perspect Biol, 2013 5(8): p. a012724. [PubMed: 23813586]
6. Fleck O and Nielsen O, DNA repair. J Cell Sci, 2004 117(Pt 4): p. 515–7. [PubMed: 14730007]
7. de Murcia G and de Murcia J. Menissier, Poly(ADP-ribose) polymerase: a molecular nick-sensor. Trends Biochem Sci, 1994 19(4): p. 172–6. [PubMed: 8016868]
8. Ray Chaudhuri A and Nussenzweig A, The multifaceted roles of PARP1 in DNA repair and chromatin remodelling. Nat Rev Mol Cell Biol, 2017 18(10): p. 610–621. [PubMed: 28676700]
9. Caldecott KW, DNA single-strand break repair. Exp Cell Res, 2014 329(1): p. 2–8. [PubMed: 25176342]
10. Caldecott KW, Single-strand break repair and genetic disease. Nat Rev Genet, 2008 9(8): p. 619–31. [PubMed: 18626472]
11. Kim MY, Zhang T, and Kraus WL, Poly(ADP-ribosyl)ation by PARP-1: ‘PAR-laying’ NAD+ into a nuclear signal. Genes Dev, 2005 19(17): p. 1951–67. [PubMed: 16140981]
12. Karanam K, et al., Quantitative live cell imaging reveals a gradual shift between DNA repair mechanisms and a maximal use of HR in mid S phase. Mol Cell, 2012 47(2): p. 320–9. [PubMed: 22841003]
13. Wright WD, Shah SS, and Heyer WD, Homologous recombination and the repair of DNA double-strand breaks. J Biol Chem, 2018 293(27): p. 10524–10535. [PubMed: 29599286]

14. Chiruvella KK, Liang Z, and Wilson TE, Repair of double-strand breaks by end joining. Cold Spring Harb Perspect Biol, 2013 5(5): p. a012757. [PubMed: 23637284]
15. Ceccaldi R, Rondinelli B, and D'Andrea AD, Repair Pathway Choices and Consequences at the Double-Strand Break. Trends Cell Biol, 2016 26(1): p. 52–64. [PubMed: 26437586]
16. Bekker-Jensen S, et al., Spatial organization of the mammalian genome surveillance machinery in response to DNA strand breaks. J Cell Biol, 2006 173(2): p. 195–206. [PubMed: 16618811]
17. Wang M, et al., PARP-1 and Ku compete for repair of DNA double strand breaks by distinct NHEJ pathways. Nucleic Acids Res, 2006 34(21): p. 6170–82. [PubMed: 17088286]
18. Rudolph J, et al., Poly(ADP-ribose) polymerase 1 searches DNA via a 'monkey bar' mechanism. Elife, 2018. 7.
19. Muthurajan UM, et al., Automodification switches PARP-1 function from chromatin architectural protein to histone chaperone. Proc Natl Acad Sci U S A, 2014 111(35): p. 12752–7. [PubMed: 25136112]
20. Figueroa-Gonzalez G and Perez-Plasencia C, Strategies for the evaluation of DNA damage and repair mechanisms in cancer. Oncol Lett, 2017 13(6): p. 3982–3988. [PubMed: 28588692]
21. Phair RD and Misteli T, Kinetic modelling approaches to in vivo imaging. Nat Rev Mol Cell Biol, 2001 2(12): p. 898–907. [PubMed: 11733769]
22. Lippincott-Schwartz J, Snapp E, and Kenworthy A, Studying protein dynamics in living cells. Nat Rev Mol Cell Biol, 2001 2(6): p. 444–56. [PubMed: 11389468]
23. Reits EA and Neefjes JJ, From fixed to FRAP: measuring protein mobility and activity in living cells. Nat Cell Biol, 2001 3(6): p. E145–7. [PubMed: 11389456]
24. Mueller F, et al., FRAP and kinetic modeling in the analysis of nuclear protein dynamics: what do we really know? Curr Opin Cell Biol, 2010 22(3): p. 403–11. [PubMed: 20413286]
25. Axelrod D, et al., Mobility measurement by analysis of fluorescence photobleaching recovery kinetics. Biophys J, 1976 16(9): p. 1055–69. [PubMed: 786399]
26. Dundr M and Misteli T, Measuring dynamics of nuclear proteins by photobleaching. Curr Protoc Cell Biol, 2003 Chapter 13: p. Unit 13 5.
27. Koster M, Frahm T, and Hauser H, Nucleocytoplasmic shuttling revealed by FRAP and FLIP technologies. Curr Opin Biotechnol, 2005 16(1): p. 28–34. [PubMed: 15722012]
28. Dittrich P, et al., Accessing molecular dynamics in cells by fluorescence correlation spectroscopy. Biol Chem, 2001 382(3): p. 491–4. [PubMed: 11347899]
29. Pramanik A, Ligand-receptor interactions in live cells by fluorescence correlation spectroscopy. Curr Pharm Biotechnol, 2004 5(2): p. 205–12. [PubMed: 15078155]
30. Maiti S, Haupts U, and Webb WW, Fluorescence correlation spectroscopy: diagnostics for sparse molecules. Proc Natl Acad Sci U S A, 1997 94(22): p. 11753–7. [PubMed: 9342306]
31. Mortusewicz O, et al., Feedback-regulated poly(ADP-ribosyl)ation by PARP-1 is required for rapid response to DNA damage in living cells. Nucleic Acids Res, 2007 35(22): p. 7665–75. [PubMed: 17982172]
32. Gong J, et al., RBM45 competes with HDAC1 for binding to FUS in response to DNA damage. Nucleic Acids Res, 2017 45(22): p. 12862–12876. [PubMed: 29140459]
33. Mani RS, et al., Domain analysis of PNKP-XRCC1 interactions: Influence of genetic variants of XRCC1. J Biol Chem, 2019 294(2): p. 520–530. [PubMed: 30446622]
34. Chen Q, et al., PARP2 mediates branched poly ADP-ribosylation in response to DNA damage. Nat Commun, 2018 9(1): p. 3233. [PubMed: 30104678]
35. Aleksandrov R, et al., Protein Dynamics in Complex DNA Lesions. Mol Cell, 2018 69(6): p. 1046–1061 e5. [PubMed: 29547717]
36. Kochan JA, et al., Meta-analysis of DNA double-strand break response kinetics. Nucleic Acids Res, 2017 45(22): p. 12625–12637. [PubMed: 29182755]
37. Izhar L, et al., A Systematic Analysis of Factors Localized to Damaged Chromatin Reveals PARP-Dependent Recruitment of Transcription Factors. Cell Rep, 2015 11(9): p. 1486–500. [PubMed: 26004182]
38. Berns MW, Rounds DE, and Olson RS, Effects of laser micro-irradiation on chromosomes. Exp Cell Res, 1969 56(2): p. 292–8. [PubMed: 5824449]

39. Krasin F and Hutchinson F, Double-strand breaks from single photochemical events in DNA containing 5-bromouracil. Biophys J, 1978 24(3): p. 645–56. [PubMed: 367461]
40. Rosenstein BS, Setlow RB, and Ahmed FE, Use of the dye Hoechst 33258 in a modification of the bromodeoxyuridine photolysis technique for the analysis of DNA repair. Photochem Photobiol, 1980 31(3): p. 215–22. [PubMed: 6154299]
41. Limoli CL and Ward JF, A new method for introducing double-strand breaks into cellular DNA. Radiat Res, 1993 134(2): p. 160–9. [PubMed: 7683818]
42. Rogakou EP, et al., Megabase chromatin domains involved in DNA double-strand breaks in vivo. J Cell Biol, 1999 146(5): p. 905–16. [PubMed: 10477747]
43. Celeste A, et al., Histone H2AX phosphorylation is dispensable for the initial recognition of DNA breaks. Nat Cell Biol, 2003 5(7): p. 675–9. [PubMed: 12792649]
44. Lukas C, et al., Distinct spatiotemporal dynamics of mammalian checkpoint regulators induced by DNA damage. Nat Cell Biol, 2003 5(3): p. 255–60. [PubMed: 12598907]
45. Lan L, et al., In situ analysis of repair processes for oxidative DNA damage in mammalian cells. Proc Natl Acad Sci U S A, 2004 101(38): p. 13738–43. [PubMed: 15365186]
46. Mortusewicz O, et al., Recruitment of RNA polymerase II cofactor PC4 to DNA damage sites. J Cell Biol, 2008 183(5): p. 769–76. [PubMed: 19047459]
47. Bradshaw PS, Stavropoulos DJ, and Meyn MS, Human telomeric protein TRF2 associates with genomic double-strand breaks as an early response to DNA damage. Nat Genet, 2005 37(2): p. 193–7. [PubMed: 15665826]
48. Dinant C, et al., Activation of multiple DNA repair pathways by sub-nuclear damage induction methods. J Cell Sci, 2007 120(Pt 15): p. 2731–40. [PubMed: 17646676]
49. Kim JS, et al., Specific recruitment of human cohesin to laser-induced DNA damage. J Biol Chem, 2002 277(47): p. 45149–53. [PubMed: 12228239]
50. Mari PO, et al., Dynamic assembly of end-joining complexes requires interaction between Ku70/80 and XRCC4. Proc Natl Acad Sci U S A, 2006 103(49): p. 18597–602. [PubMed: 17124166]
51. Chen BP, et al., Cell cycle dependence of DNA-dependent protein kinase phosphorylation in response to DNA double strand breaks. J Biol Chem, 2005 280(15): p. 14709–15. [PubMed: 15677476]
52. Kong X, et al., Comparative analysis of different laser systems to study cellular responses to DNA damage in mammalian cells. Nucleic Acids Res, 2009 37(9): p. e68. [PubMed: 19357094]
53. Bao Y and Shen X, Chromatin remodeling in DNA double-strand break repair. Curr Opin Genet Dev, 2007 17(2): p. 126–31. [PubMed: 17320375]
54. Peterson CL and Cote J, Cellular machineries for chromosomal DNA repair. Genes Dev, 2004 18(6): p. 602–16. [PubMed: 15075289]
55. Kruhlak MJ, et al., Changes in chromatin structure and mobility in living cells at sites of DNA double-strand breaks. J Cell Biol, 2006 172(6): p. 823–34. [PubMed: 16520385]
56. Strickfaden H, et al., Poly(ADP-ribosyl)ation-dependent Transient Chromatin Decondensation and Histone Displacement following Laser Microirradiation. J Biol Chem, 2016 291(4): p. 1789–802. [PubMed: 26559976]
57. Kong X, et al., Biphasic recruitment of TRF2 to DNA damage sites promotes non-sister chromatid homologous recombination repair. J Cell Sci, 2018 131(23).
58. Smith R and Timinszky G, Monitoring Poly(ADP-Ribosyl)ation in Response to DNA Damage in Live Cells Using Fluorescently Tagged Macrodomains. Methods Mol Biol, 2018 1813: p. 11–24. [PubMed: 30097858]
59. Morotomi-Yano K, et al., Dynamic behavior of DNA topoisomerase IIbeta in response to DNA double-strand breaks. Sci Rep, 2018 8(1): p. 10344. [PubMed: 29985428]
60. Polo LM, et al., Efficient Single-Strand Break Repair Requires Binding to Both Poly(ADP-Ribose) and DNA by the Central BRCT Domain of XRCC1. Cell Rep, 2019 26(3): p. 573–581 e5. [PubMed: 30650352]
61. Tampere M and Mortusewicz O, DNA Damage Induction by Laser Microirradiation. Bioprotocol, 2016 6(23): p. e2039.

62. Xie S, et al., Timeless Interacts with PARP-1 to Promote Homologous Recombination Repair. Mol Cell, 2015 60(1): p. 163–76. [PubMed: 26344098]
63. Sellou H, et al., The poly(ADP-ribose)-dependent chromatin remodeler Alc1 induces local chromatin relaxation upon DNA damage. Mol Biol Cell, 2016 27(24): p. 3791–3799. [PubMed: 27733626]
64. Mahadevan J, et al., Q-FADD: A Mechanistic Approach for Modeling the Accumulation of Proteins at Sites of DNA Damage. Biophys J, 2019 116(11): p. 2224–2233. [PubMed: 31109734]
65. Karanam K, Loewer A, and Lahav G, Dynamics of the DNA damage response: insights from live-cell imaging. Brief Funct Genomics, 2013 12(2): p. 109–17. [PubMed: 23292635]
66. Fay DS and Gerow K, A biologist's guide to statistical thinking and analysis. WormBook, 2013: p. 1–54.
67. Lukas C, et al., Mdc1 couples DNA double-strand break recognition by Nbs1 with its H2AX-dependent chromatin retention. EMBO J, 2004 23(13): p. 2674–83. [PubMed: 15201865]
68. Bekker-Jensen S, et al., Dynamic assembly and sustained retention of 53BP1 at the sites of DNA damage are controlled by Mdc1/NFBD1. J Cell Biol, 2005 170(2): p. 201–11. [PubMed: 16009723]
69. Mayer J, Khairy K, and Howard J, Drawing an elephant with four complex parameters. American Journal of Physics, 2010 78(6): p. 648–649.
70. Kong M, et al., Single-Molecule Imaging Reveals that Rad4 Employs a Dynamic DNA Damage Recognition Process. Mol Cell, 2016 64(2): p. 376–387. [PubMed: 27720644]
71. Friis I and Solov'yov IA, Activation of the DNA-repair mechanism through NBS1 and MRE11 diffusion. PLOS Computational Biology, 2018 14(7): p. e1006362. [PubMed: 30052627]
72. Mazza D, et al., A benchmark for chromatin binding measurements in live cells. Nucleic Acids Res, 2012 40(15): p. e119. [PubMed: 22844090]
73. Hinow P, et al., The DNA binding activity of p53 displays reaction-diffusion kinetics. Biophys J, 2006 91(1): p. 330–42. [PubMed: 16603489]
74. Gibbs-Seymour I, et al., HPF1/C4orf27 Is a PARP-1-Interacting Protein that Regulates PARP-1 ADP-Ribosylation Activity. Mol Cell, 2016 62(3): p. 432–442. [PubMed: 27067600]
75. Bonfiglio JJ, et al., Serine ADP-Ribosylation Depends on HPF1. Mol Cell, 2017 65(5): p. 932–940 e6. [PubMed: 28190768]
76. Kozlowski M, The molecular mechanism of PARP1 activation and its downstream roles in ALC1-regulated transcription. 2014.
77. Toseland CP, Fluorescent labeling and modification of proteins. J Chem Biol, 2013 6(3): p. 85–95. [PubMed: 24432126]
78. Crivat G and Taraska JW, Imaging proteins inside cells with fluorescent tags. Trends Biotechnol, 2012 30(1): p. 8–16. [PubMed: 21924508]
79. Carrero G, et al., Using FRAP and mathematical modeling to determine the in vivo kinetics of nuclear proteins. Methods, 2003 29(1): p. 14–28. [PubMed: 12543068]
80. Phair RD, Gorski SA, and Misteli T, Measurement of dynamic protein binding to chromatin in vivo, using photobleaching microscopy. Methods Enzymol, 2004 375: p. 393–414. [PubMed: 14870680]
81. Kaufman EN and Jain RK, Quantification of transport and binding parameters using fluorescence recovery after photobleaching. Potential for in vivo applications. Biophys J, 1990 58(4): p. 873–85. [PubMed: 2248992]
82. Nenninger A, Mastroianni G, and Mullineaux CW, Size dependence of protein diffusion in the cytoplasm of Escherichia coli. J Bacteriol, 2010 192(18): p. 4535–40. [PubMed: 20581203]
83. Leonard Kaufman PJR, Finding Groups in Data: An Introduction to Cluster Analysis. 2008.
84. MacQueen J Some methods for classification and analysis of multivariate observations In Proceedings of the Fifth Berkeley Symposium on Mathematical Statistics and Probability, Volume 1: Statistics. 1967 Berkeley, Calif.: University of California Press.
85. Ester M, et al., A density-based algorithm for discovering clusters a density-based algorithm for discovering clusters in large spatial databases with noise, in Proceedings of the Second

International Conference on Knowledge Discovery and Data Mining 1996, AAAI Press: Portland, Oregon p. 226–231.

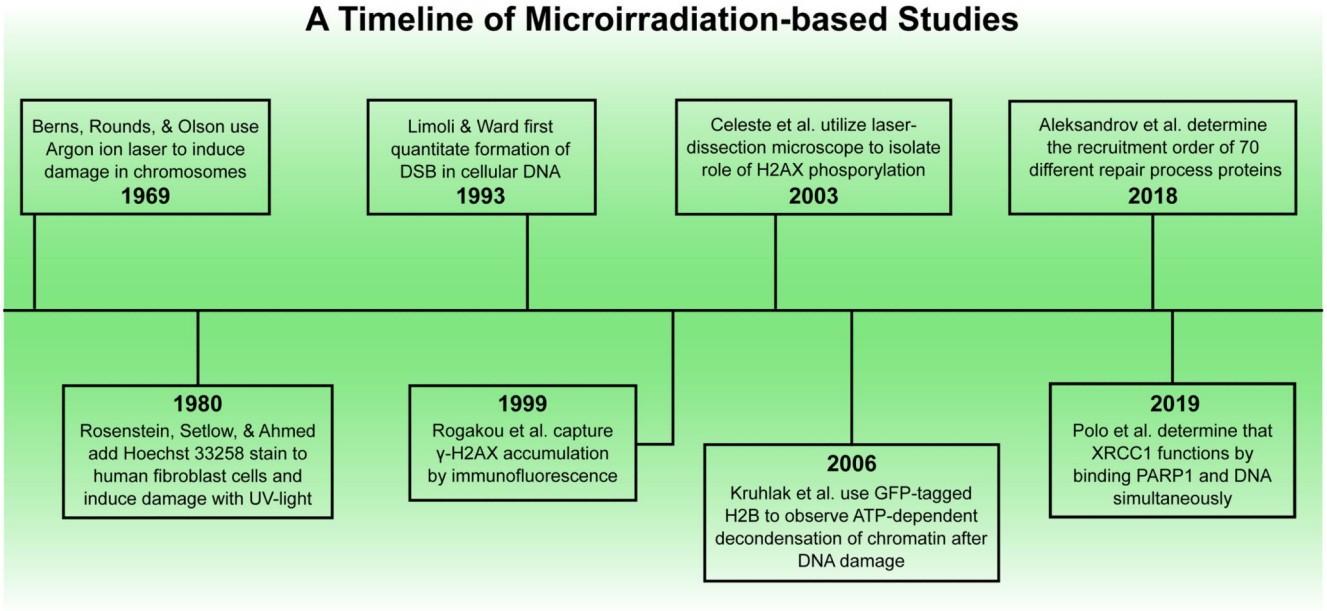

Figure 1.

Timeline of DNA microirradiation studies. While this timeline is not exhaustive, it highlights a few of the many significant microirradiation experiments over the 50-year history of the field.

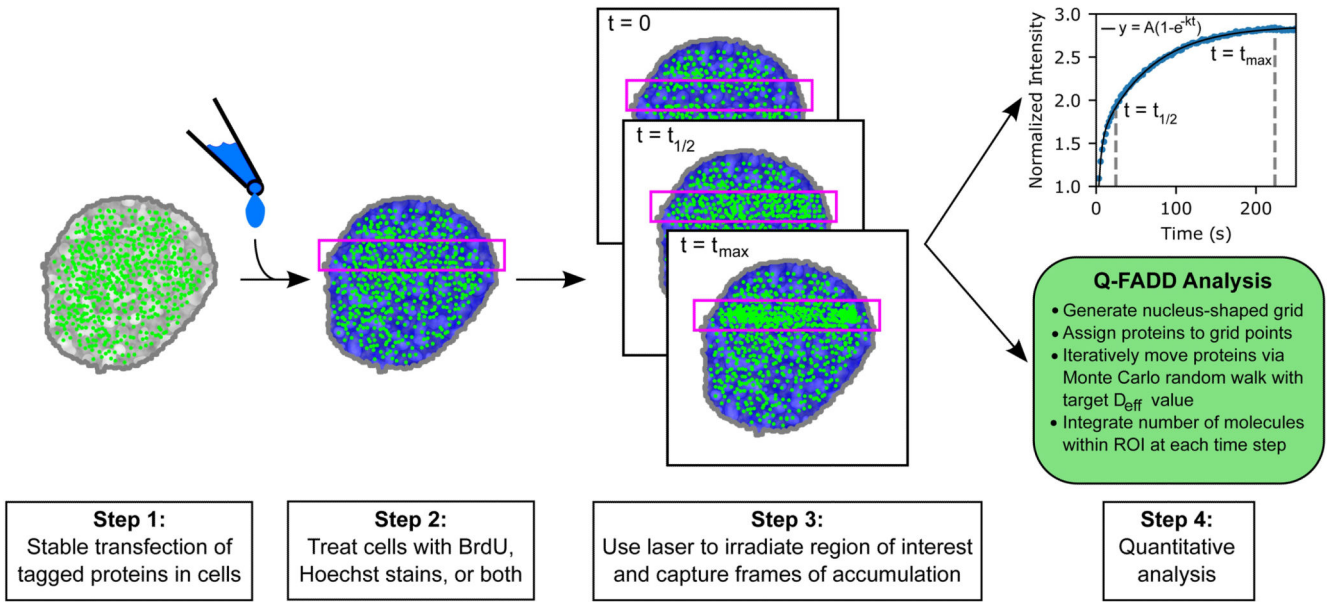

Figure 2.

A schematic of the microirradiation measurement and analysis workflow. First, cells are transfected with a vector containing the fluorescently labeled protein of interest. Then, cells may be pre-sensitized for DNA damage by the introduction of BrdU, Hoechst dyes, or both. After pre-sensitization, cells are placed in a confocal microscope and microirradiated with a laser beam, producing a region-of-interest (ROI) across the length of the cell (as shown above). Immediately preceding and following microirradiation, accumulation of labeled repair proteins to DNA lesions in the ROI is captured by live images over a set course of time. These images are then analyzed and converted to a fluorescence intensity timeseries, which is fit using the techniques described in Section 3.

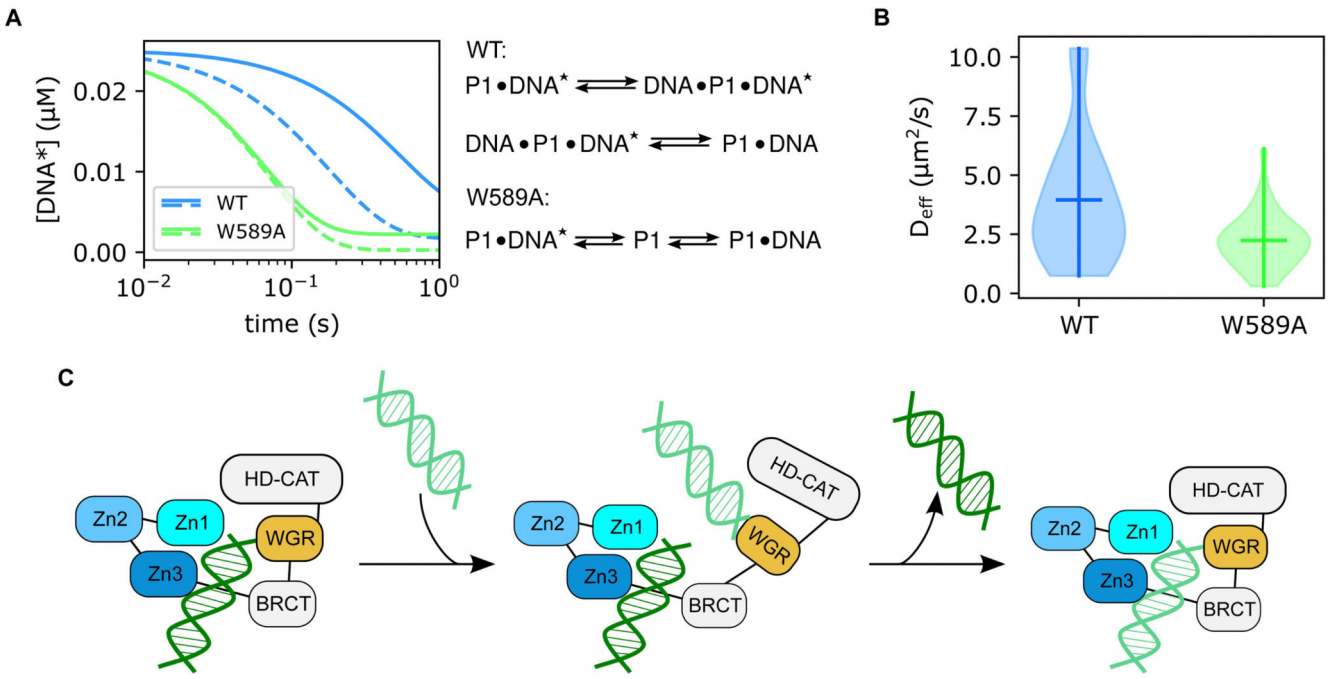

Figure 3.

The "monkey bar" mechanism of PARP1 mobility. (A) Stopped-flow kinetics models show that wild-type PARP1 (blue) releases pre-bound DNA fragments ([DNA*]) at a significantly slower rate than the W589A mutant (green). The W589A mutant showed no difference in off-rate observation between low A Timeline of Microirradiation-based Studies(0.4 μM, solid line) and high (4 μM, dashed line) concentrations of competitor DNA, but wild-type PARP1 displays faster release of the initially bound strand when exposed to a higher concentration of competitor DNA. In addition, fitting of W589A kinetics were adequately described by a two-state equation, whereas wild-type data required formation of an intermediate state. (B) Violin plots of modeled D_{eff} values from Q-FADD analyses on wild-type (blue) and W589A (green) microirradiation data. These models show that wild-type PARP1 diffuses significantly more quickly to DNA lesions than the W589A mutant (p-value = 0.0094). (C) Graphical representation of the "monkey bar" mechanism derived from the combination of these data. The WGR domain of PARP1 releases from the currently bound DNA strand and binds to a neighboring strand of DNA, then the original strand of DNA is released and the complex collapses around the newly bound DNA fragment. Figures were adapted from our published (free-access) data [18].